Pure appl. geophys. 159 (2002) 831–863
0033–4553/02/040831–33 $ 1.50 + 0.20/0

Pure and Applied Geophysics

Identification of Mining Blasts at Mid- to Far-regional Distances Using Low Frequency Seismic Signals

MICHAEL A. H. HEDLIN,[1] BRIAN W. STUMP,[2,3] D. CRAIG PEARSON,[3] and XIAONING YANG[3]

Abstract—This paper reports results from two recent monitoring experiments in Wyoming. Broadband seismic recordings of kiloton class delay-fired cast blasts and instantaneous calibration shots in the Black Thunder coal mine were made at four azimuths at ranges from 1° to 2°. The primary focus of this experiment was to observe and to explain low-frequency signals that can be seen at all azimuths and should routinely propagate above noise to mid-regional distances where most events will be recorded by International Monitoring System (IMS) stations.

The recordings clearly demonstrate that large millisecond delay-fired cast blasts routinely produce seismic signals that have significant spectral modulations below 10 Hz. These modulations are independent of time, the azimuth from the source and the orientation of the sensor. Low-frequency modulations below 5 Hz are seen beyond 9°. The modulations are not due to resonance as they are not produced by the calibration shots. Linear elastic modeling of the blasts that is guided by mine-blast reports fails to reproduce the fine detail of these modulations but clearly indicates that the enhanced "spectral roughness" is due to long interrow delays and source finiteness. The mismatch between the data and the synthetics is likely due to source processes, such as nonlinear interactions between shots, that are poorly understood and to other effects, such as variations of shot time and yield from planned values, that are known to be omnipresent but cannot be described accurately. A variant of the Automated Time-Frequency Discriminant (HEDLIN, 1998b), which uses low-frequency spectral modulations, effectively separates these events from the calibration shots.

The experiment also provided evidence that kiloton class cast blasts consistently yield energetic 2–10 second surface waves. The surface waves are strongly dependent on azimuth but are seen beyond 9°. Physical modeling of these events indicates that the surface waves are due mainly to the extended source duration and to a lesser extent to the slap-down of spalled material. The directionality is largely a path effect. A discriminant that is based on the partitioning of energy between surface and body waves routinely separates these events from the calibration shots.

The Powder River Basin has essentially no natural seismic activity. How these mining events compare to earthquake observations remains to be determined.

Key words: Spectral modulations, attenuation, surface waves, remote source characterization.

1. Introduction

The recent Comprehensive Nuclear-Test-Ban Treaty (CTBT) is unlike any earlier test ban accord, such as the Threshold Test-Ban Treaty (TTBT) which prohibits tests

[1] IGPP-University of California, San Diego, La Jolla, CA, 92093-0225, U.S.A.
[2] Southern Methodist University, U.S.A.
[3] Los Alamos National Laboratory, U.S.A.

above 150 kilotons, as it bans nuclear explosions of any yield. The exclusive nature of this treaty and the fact that a 1 kiloton contained explosion in hard rock is well above magnitude 4 motivates interest in the accurate characterization of small ($m_b < 4.0$) seismic events (MURPHY, 1995). Detonating a nuclear explosion in a cavity can further reduce the magnitude of the seismic waves (U.S. CONGRESS, OTA REPORT, 1988). Interest in small events has increased both the numbers of events that must be considered and the types. It is estimated that, globally, 21,000 events with m_b above 3.5 occur per year (U.S. CONGRESS OTA REPORT; p. 78). Some of these small events will not be associated with natural seismic activity but are due to commercial blasting which occurs globally. The blasting technique favored worldwide is delay firing (LANGEFORS and KIHLSTRÖM, 1978) in which a number of charges are arranged in a spatial grid and detonated in sequence. This technique is favored as it yields efficient fracturing of rock while minimizing damaging seismic and acoustic signals in areas proximal to the mine. Commercial blasting is common but usage varies widely (LEITH, 1994). KHALTURIN *et al.* (1997) surveyed over 30 regions worldwide and found that several hundred industrial blasts each year have a magnitude greater than 3.5. Large blasts, often associated with construction, were relatively common in the Former Soviet Union and in China however the current blasting practice is not yet well known (Bill Leith, personal communication). In Wyoming, very large (>1 kt) surface coal mine blasts are common. The Black Thunder coal mine, one of several mines in the Powder River Basin in NE Wyoming, typically detonates 1 to 2 blasts of this magnitude each month (PEARSON *et al.*, 1995; STUMP, 1995) with a few in the magnitude range of 3.5 to above 4.0.

The Reviewed Event Bulletin (REB), published by the prototype International Data Centre (PIDC), indicates that large mining explosions are commonly detected by IMS seismic stations at all regional distances; some are seen teleseismically. Although there has been very promising progress in identifying mine blasts using correlation techniques (HARRIS, 1991; ISRAELSON, 1991; RIVIERE-BARBIER and GRANT, 1993), significant changes in how mine blasts are detonated at an individual mine are known to occur (MARTIN *et al.*, 1997). This gives us the impetus for exploring other, complimentary, methods. Large mining events are problematic not just because these events will trigger the IMS, but these large, controlled, explosions offer a means to obscure nuclear tests. The "hide-in-quarry blast" evasion scenario (BARKER and DAY, 1990; BARKER *et al.*, 1994; RICHARDS and ZAVALES, 1990; SMITH, 1993), in which a nuclear test is colocated with a mining blast, might be troubling because blasting anomalies, in which a large part of a mining explosion shot grid detonates simultaneously, are not uncommon (MARTIN *et al.*, 1997). A nuclear test colocated with an industrial explosion might be entirely hidden or mistaken for a detonation anomaly.

The CTBT calls for an International Monitoring System (IMS) which will comprise four networks of sensors (seismic, infrasound, radionuclide and hydroacoustic). The seismic network will consist of 50 primary stations and over 100

secondary stations (Fig. 1). This network will place a station within local distance (1°) of 2% of the Earth's landmass. The near-regional (within 5°) coverage will be 34%. The mid-regional coverage (within 15° of the source) is nearly complete at 89% (Fig. 2). If multiple recordings are required for accurate source characterization, the coverage is more limited. Just 22% of the Earth's landmass is within 10° of 3 stations; 74% is within 20°. Some prominent mining regions (e.g., the Kuzbass/Abakan mining region in Russia near the IMS station ZAL) will be monitored at near-regional range (Fig. 2) and a full suite of high- and low-frequency characterization techniques can be brought to bear on suspicious events (STUMP *et al.*, 1999a). In many regions, however, monitoring of man-made and natural seismic activity will rely on recordings made at mid- to far-regional range. Events in these regions will require a more limited set of seismic discriminants: those that operate at low frequencies. Although millisecond delay-fired industrial explosions will produce diagnostic spectral peaks at high frequency, because of interference between shots, the industry standard intershot time delay is 35 msec and the resulting spectral peak is at ~30 Hz (the inverse of the intershot time delay). As the standard sampling rate for IMS stations is 40 samples/sec (sps), this energy will lie beyond the Nyquist frequency of most recordings that will be made under the CTBT.

Quantitative detection capability of the IMS involves many factors, including spatial decay rates, event size, noise levels, instrument type (e.g., array, single station), and phase (e.g., *P* and *S*). There have been many studies quantifying these into the detection capability of the IMS (e.g., WUSTER *et al.*, 2000). The analysis in

Figure 1
Distribution of current and proposed primary (red) and auxiliary (yellow) IMS seismic stations. Array sites and three-component stations are represented as circles and triangles, respectively. Additional stations (in black) are in the IRIS GSN. A regional network considered in this study was deployed in Wyoming and is represented by the oval.

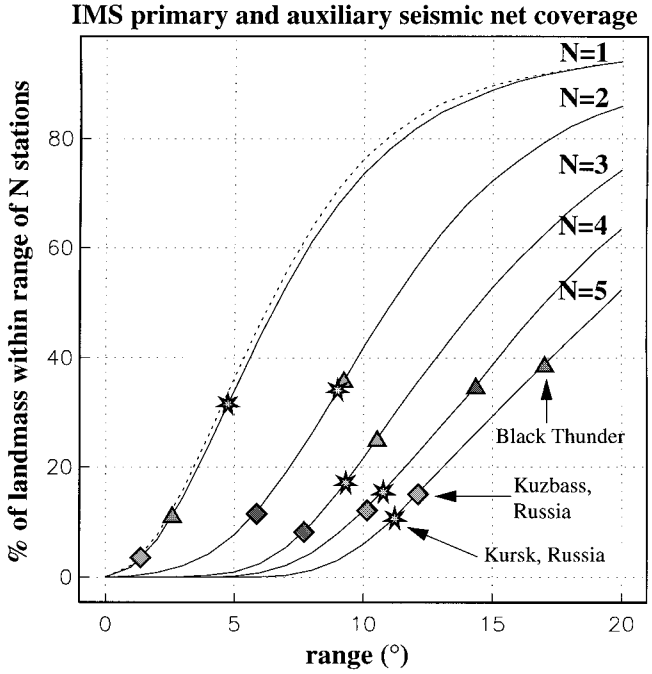

Figure 2

Coverage of the Earth's landmass permitted by the current and proposed IMS primary and secondary seismic networks is indicated by the solid curves. Single-station coverage ($N = 1$) is nearly complete within 10° of the source. If multiple recordings of an event are required for adequate source characterization ($N > 1$), most of the observations will be made at mid- to far-regional or teleseismic range. Coverage of three prominent mining regions is indicated by shaded symbols. Krasnogorsky, the main Kuzbass mine in Russia, at 53.6°N, 87.8°E; Black Thunder in Wyoming at 43.7°N, 105.25°W and Kursk, Russia at 51.8°N, 36.5°E are represented by diamonds, triangles and stars, respectively. These mining regions will be monitored somewhat more closely than the average. For example, three stations are within 8° of the Kuzbass mine. Just 8% of the Earth's landmass has better coverage. The dashed curve is coverage given by the IMS networks (current and proposed) and existing stations in the GSN. Many stations in the GSN that are not already in the IMS are located on oceanic islands and so the improvement is limited.

this case is to emphasize the distance range at which observations of mining explosions are most likely to be made.

It is apparent that large blasts emit seismic energy which can be used for source characterization from local to far-regional distances. Spectral modulations below 10 Hz have been observed by several groups (incl., BAUMGARDT and ZIEGLER, 1988) and are usually attributed to long intershot, or interrow, delays. GITTERMAN and VAN ECK (1993) attributed a low frequency spectral notch in recordings of mine blasts to source finiteness. Unusual time-domain characteristics also have been observed. ANANDAKRISHNAN *et al.* (1997) and STUMP and PEARSON (1997) observed significant surface waves caused by cast explosions in Wyoming. GITTERMAN *et al.* (1997) observed surface waves in recordings of quarry blasts in Israel. ANANDAKRISHNAN

et al. (1997) modeled the Wyoming blasts and concluded that the surface waves are due to long source duration and significant spall, including material cast into the pit.

This paper presents further evidence for significant seismic signals produced by large mining blasts and not by instantaneous explosions. The paper presents evidence for spectral modulations below 10 Hz produced by documented (''ground truthed'') cast blasts in Wyoming. Low-frequency modulations, below 5 Hz, are seen at an IMS station at a range of 9°. The paper identifies observations of significant surface waves also produced just by these events. Source modeling is used to understand these observations and to gauge the sensitivity of these signals to changes in blasting parameters at the source. We assess the usefulness of these signals, and low-frequency spectral modulations, for characterizing mining explosions using the IMS.

2. Regional Monitoring Experiments in Wyoming

To investigate low-frequency seismic signals produced by large mining blasts, researchers from the University of California, San Diego (UCSD), in collaboration with researchers from the Los Alamos National Laboratory (LANL), Southern Methodist University (SMU) and the Air Force Technical Applications Center (AFTAC), conducted two regional monitoring experiments in Wyoming in 1996 and 1997. Five broadband three-component seismic stations (STS-2's; flat response from 0.0083 to 40 Hz) were deployed within near-regional range of the Black Thunder mine (Fig. 3). Four of the sensors were deployed in a ring at 200-km range to study the azimuthal dependence of the seismic signals. The fifth station was deployed (in 1996) at a range of 100 km to the north of the mine along the azimuth to station CUST to allow examination of the range dependence. A three-element, 100-m aperture infrasound array was deployed at station MNTA (Fig. 3). The temporary deployments complemented permanent, nearby, deployments at PDAR, RSSD and more distant stations in the IMS and the IRIS Global Seismographic Network (GSN).

The seismic activity in this region is almost entirely man-made and is concentrated in the Powder River Basin coal mining trend (Fig. 3). Two types of blasting are most common in this trend. The largest blasts are used to cast overburden to the side to expose the coal seam (MARTIN and KING, 1995). Smaller shots are used to fracture the coal seam to facilitate recovery (ATLAS POWDER COMPANY, 1997). Event clusters correlate well with known mine locations (Fig. 3). The events of greatest interest were the large cast blasts and calibration shots, located in the Black Thunder coal mine (PEARSON *et al*., 1995; STUMP, 1995), as these were closely monitored with video and acoustic equipment by the LANL team and were carefully documented by personnel at the mine. During the two experiments, four large cast blasts were detonated at Black Thunder (Fig. 4; Table 1). These blasts ranged from 2.5 million pounds (Aug. 1, 1996) to 7 million pounds (Aug. 14, 1997) and were used to move overburden. Three of four blasts occurred in the south pit of

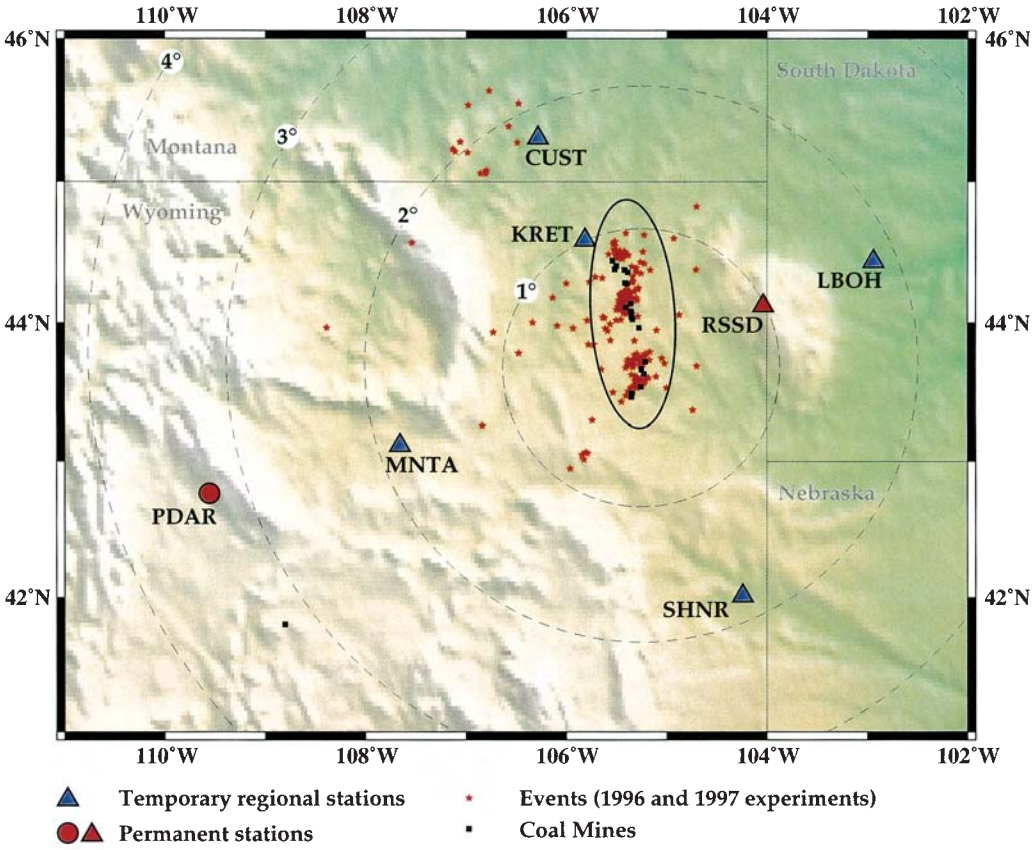

Figure 3
Two regional experiments were conducted in Wyoming by LANL, SMU, AFTAC and UCSD in 1996 and 1997. Four broadband seismic stations (three-component STS2's) were deployed in a ring surrounding the Powder River Basin (PRB) at a range of 200 km from the Black Thunder coal mine. A fifth station (KRET) was deployed at a range of 100 km. Permanent seismic stations are located at PDAR and RSSD. Infrasound sensors were deployed at MNTA. Mining explosions detected by the temporary seismic stations during 49 days in 1996 and 1997 are plotted and correlate well with known mines. The slight northward bias is likely due to the 1-D model. The oval indicates approximate limits of the PRB.

Black Thunder where overburden is cast to the north. Typical cast blasts include several (typically ~7) rows of shots. Intershot time spacing is 35 msec, rows are spaced by 200 to 300 msec. For reasons as yet not fully understood, one cast blast (Aug. 1, 1996) detonated, in part, nearly simultaneously. Six calibration shots (ranging from 5000 to 16,000 pounds) were detonated in the mine in 1997 (Fig. 4; Table 2). The first four calibration shots (yields 5000 to 5500 pounds) consisted of a single cylindrical borehole. The fifth and sixth calibration shots (yields 12,000 and 16,000 pounds) consisted of 3 and 4 boreholes, respectively. The boreholes in the larger shots were spaced 20 to 30 m apart and detonated simultaneously. In the

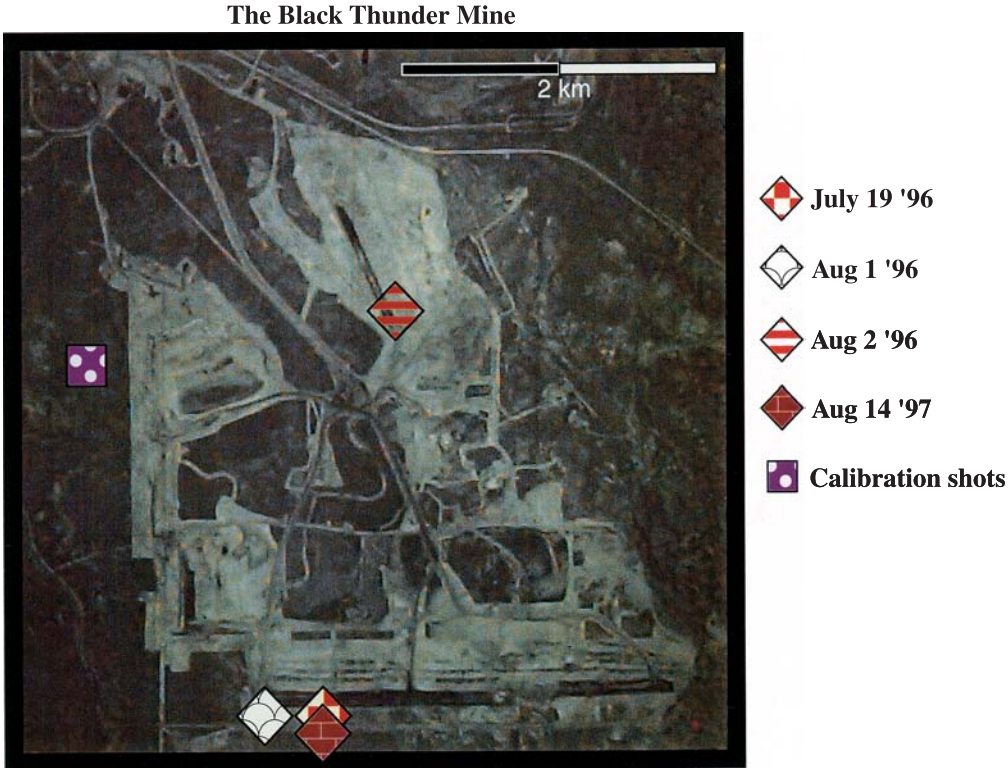

Figure 4
A satellite photo of the Black Thunder coal mine in Wyoming. The symbols give approximate locations of the major events considered in this paper. The 1996 and 1997 experiments produced recordings of four significant cast blasts in the Black Thunder coal mine. The July 19, Aug. 1, 1996 and Aug. 14, 1997 blasts occurred at the west end of the south pit. The west end of the Aug. 1 blast is believed to have detonated simultaneously. In the July 19, Aug. 1, 2 (all 1996) and Aug. 14 (1997) cast blasts 4.5, 2.5, 2.8 and 7.0 million pounds of ANFO were detonated. The two largest calibration tests involved 12,000 and 16,000 pounds of ANFO.

Table 1

Major blasts at Black Thunder

Date	Pit/firing direction	# Rows/# holes	Intershot/interrow delays (m_s)	Total explosive yield (pounds)
July 19, 1996	South/west	7/620 (decked)	35/200–275	4,549,366
Aug. 1, 1996	South/west	7/341	35/200–275	2,460,730
Aug. 2, 1996	NE/south	7/422	35/200–275	2,784,540
Aug. 14, 1997	South/west	7/702	35/200–400	5,958,010

Table 2

Calibration shots at Black Thunder in 1997

Date	Yield (pounds)
Aug. 14, 1997	~5500
Aug. 14, 1997	~5500
Aug. 14, 1997	~5500
Aug. 14, 1997	~6000
Aug. 15, 1997	~12,000
Aug. 15, 1997	~16,000

discussion that follows, we consider the time and frequency domain characteristics of all large Black Thunder events that occurred during the two experiments. However, we will focus on two events; the 4.5 million pound cast blast that occurred on July 19, 1996 and the 16,000 pound calibration shot.

3. Observations of Low-frequency Seismic Signals from Mining Blasts

Time Domain Energy Partitioning

Amplitudes of body waves produced by the 4.5 million pound July 19 cast blast are comparable to those produced by the 16,000 pound calibration shot (Fig. 5). This is expected as the July 19 blast yield is spread out over 620 shots which were arranged in 7 rows and ripple-fired over ~4.8 s. Each shot hole was decked – that is two explosive charges were detonated with a small delay in each hole. Although the two events produced similar body waves, just the cast shot produced significant surface waves (Fig. 5). Unfiltered recordings of the July 19 blast (Fig. 6) show the progression from high-frequency body waves to low-frequency surface waves at four azimuths. The surface-wave amplitudes exhibit a clear dependence on azimuth. Figure 7 indicates that although the low-frequency waveforms are highly dependent on azimuth, these signals do not seem to depend strongly on the fine details of the source if the blasts are in the same pit.

ANANDAKRISHNAN *et al.* (1997) and STUMP and PEARSON (1997) have published PDAR recordings of significant 4 to 12 second surface waves which are produced by cast blasts in Wyoming. ANANDAKRISHNAN *et al.* (1997) used linear source modeling to argue that the surface waves are the result of the long source duration and spall impacts. The 1996 and 1997 regional experiments indicate that these surface waves are routinely produced by the cast explosions and are readily detected at near-regional range.

In Figure 8, peak amplitudes in two pass bands (1 to 10 Hz; centered at *P* onset and 2 to 10 seconds centered on the surface wave) are estimated from noise-corrected envelopes of recordings made by the stations in the 200-km ring (Fig. 3). The cast blasts and calibration explosions are easily separated despite the strong

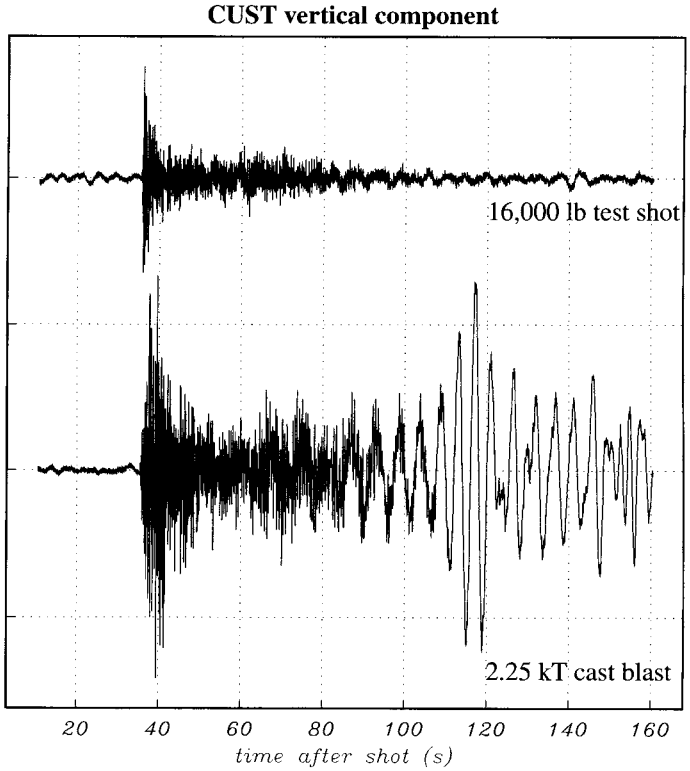

Figure 5
Unfiltered vertical component recordings of a 16,000 pound calibration shot (top) and a 4.5 million pound cast shot made at CUST. Both recordings are plotted at the same scale. The station was located 200 km to the north of the events (Fig. 3) which occurred in the Black Thunder coal mine. The tiny calibration shot rivals the immense cast shot as a source of *P* waves but is an insignificant source of surface waves. The dissimilarity of unfiltered vertical component recordings made at CUST is consistent with previous findings (KIM *et al.*, 1994; ANANDAKRISHNAN *et al.*, 1997) and suggests that a regional variant of the M_S:m_b discriminant could be effective for separating large mine blasts from instantaneous explosions.

dependence of the peak surface-wave amplitudes on azimuth. Although small calibration shots yield *P* waves that are comparable in strength to those produced by the much larger, but not concentrated, cast blasts, just the latter events produce significant surface waves. As indicated in this figure, the calibration shots yielded no surface-wave energy above noise. The lone outlier, among the population of cast blasts, is the Aug. 1, 1996 event. A significant simultaneous detonation, which occurred within this blast, significantly boosted peak *P*-wave amplitudes. The network average surface-wave amplitudes are almost identical, despite the significant differences in how these blasts were detonated. Despite the boosted *P*-wave amplitudes observed in the Aug. 1, 1996 recordings, the amplitude ratio comparing surface waves to body waves still separates this event from the single shots.

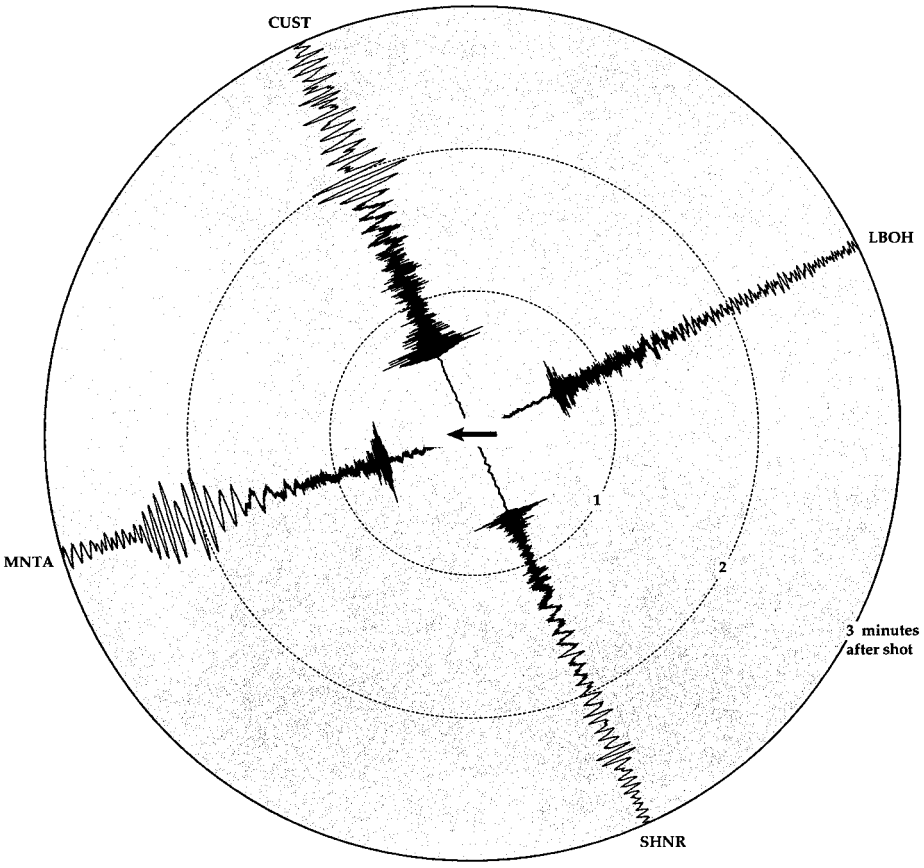

Figure 6
Unfiltered vertical component seismograms from the azimuthal network show the progression from high-frequency body waves to substantial surface waves. The July 19, 1996 blast used 4.5 million pounds of ANFO which detonated as planned. The arrow indicates the direction of shooting. The waveforms are highly dependent on azimuth. Propagation to the east across the Black Hills Pluton resulted in relatively little surface-wave energy.

Frequency Domain Modulations

Previous studies (incl. STUMP and PEARSON, 1997) have shown that the large cast explosions in Wyoming do not yield obvious spectral modulations above 10 Hz. The intershot delays of 35 msec concentrate energy at multiples of 29 Hz (1/0.035 s). Close-in data show a spectral increase that corresponds to the 35 ms delays although the peak is relatively broad, reflective of the different spatial locations of the individual charges and possibly variance in their individual detonation time. Rapid attenuation in this area is an additional cause of the faintness of the high-frequency modulations. These explosions do, however, produce significant modulations below

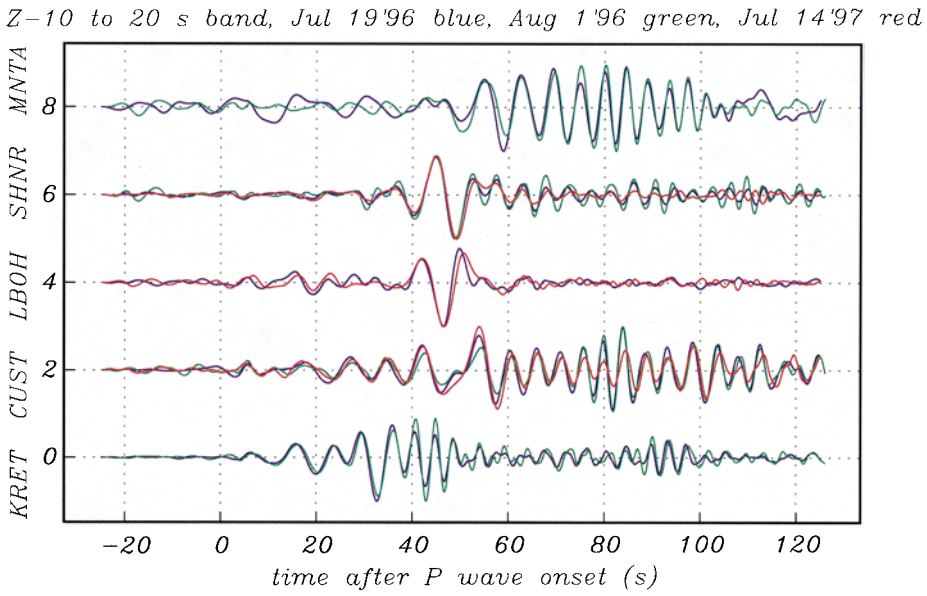

Figure 7
A comparison of band-pass filtered regional seismograms from three different cast blasts at five different stations at varying azimuths from the mine (see Fig. 3). All of these blasts occurred in the south pit of the Black Thunder coal mine. All shots were detonated in the south pit of the Black Thunder coal mine (Fig. 4). Low-frequency seismic signals from the south pit events are robust although highly dependent on azimuth.

10 Hz. Spectral estimates taken from recordings of the July 19, 1996 cast blast made by the 5 station regional network are shown in Figures 9 and 10. These spectra exhibit only a modest dependence on time, the recording direction, and the azimuth from the mine. No organized spectral modulations are seen in the recordings of any of the calibration shots. In this figure we display spectra from the 16,000 pound shot (dashed curves). As will be seen later, the low-frequency modulations below 5 Hz are seen out to 9°.

4. *Waveform Synthesis*

To give these basic observations a physical basis, we turn to synthetics. The synthesis of extraordinarily complex mining explosions has become relatively easy given the early work of BARKER and DAY (1990), BARKER *et al.* (1993) and MCLAUGHLIN *et al.* (1994) and recent work by X. Yang who has modified the linear elastic algorithm of ANANDAKRISHNAN *et al.* (1997) and packaged it into an interactive MATLAB package (MineSeis; YANG, 1998). The algorithm assumes the linear superposition of signals from identical single-shot sources composed of

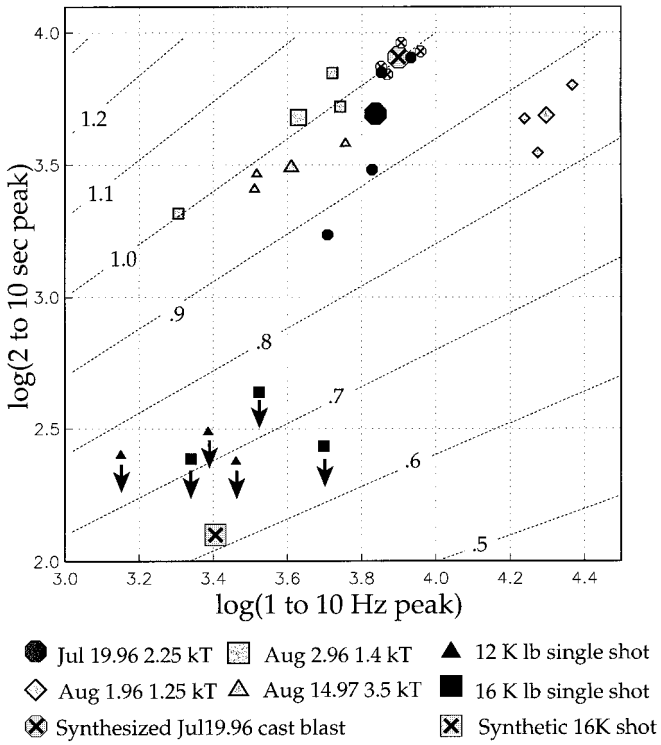

Figure 8
A comparison of 2 to 10 second surface wave and 1 to 10 Hz *P*-wave peak amplitudes using recordings made at a range of 200 km by MNTA, CUST, LBOH & SHNR (Fig. 3). All events occurred in the Black Thunder coal mine. Each trace is filtered, converted to an envelope and adjusted downward by an amount determined by pre-onset noise. Above are displayed the logarithms of the individual station peak amplitudes. The large symbols represent the network average for each event. Each labeled curve indicates a constant ratio of surface wave to *P*-wave amplitude [i.e. log(2 to 10 s peak)/log(1 to 10 Hz peak)]. As expected the calibration shots yield essentially no surface-wave energy above noise. The downward arrows indicate that the maximum *P*-wave amplitude is well constrained but the surface-wave amplitude lies below noise. For this reason, no network averages are displayed for these events. The Aug. 1, 1996 cast shot appears as being somewhat explosion-like due to the sympathetic detonation. The sympathetic detonation greatly boosted *P*-wave amplitudes but left the surface waves untouched. Unadjusted amplitudes are plotted as all stations are at the same range from the mine. We also display peak amplitudes from a synthetic version of the July 19 cast blast and from a synthetic 16,000 pound calibration shot. The energy partitioning from the synthetic events is in agreement with observations.

isotropic and spall components. Both shooting delays and location differences among individual shots are taken into account in calculating delays of the superposition, although the Green's functions are assumed to change slowly so that a common Green's function is used for all the single shots. We used a reflectivity method to calculate the Green's functions. A one-dimensional velocity model was used (PRODEHL, 1979; ANANDAKRISHNAN *et al.*, 1997).

To model the July 19 cast blast we used a blast report issued by the Black Thunder mine. The blast consisted of 7 rows and a total of 620 decked shots with a total yield of 4.5 million pounds (Table 1). In a decked shot, more than one charge is detonated in the same hole. In this event, each hole contained two charges separated by 50 to 200 msec. Although the number of shots in each row varied from 85 to 93, for simplicity we assumed each row had 89 shots and that each decked shot had a total yield of 0.0033 kt. We assumed that all rows were spaced by 9.1 m and that all adjacent shots in the same row were 10.4 m apart. Intershot delays were 35 msec, interrow delays ranged from 200 to 275 msec. SOBEL (1978) estimated that 9.6×10^9 kg of material is spalled by each kt detonated. In our experiment, each decked shot

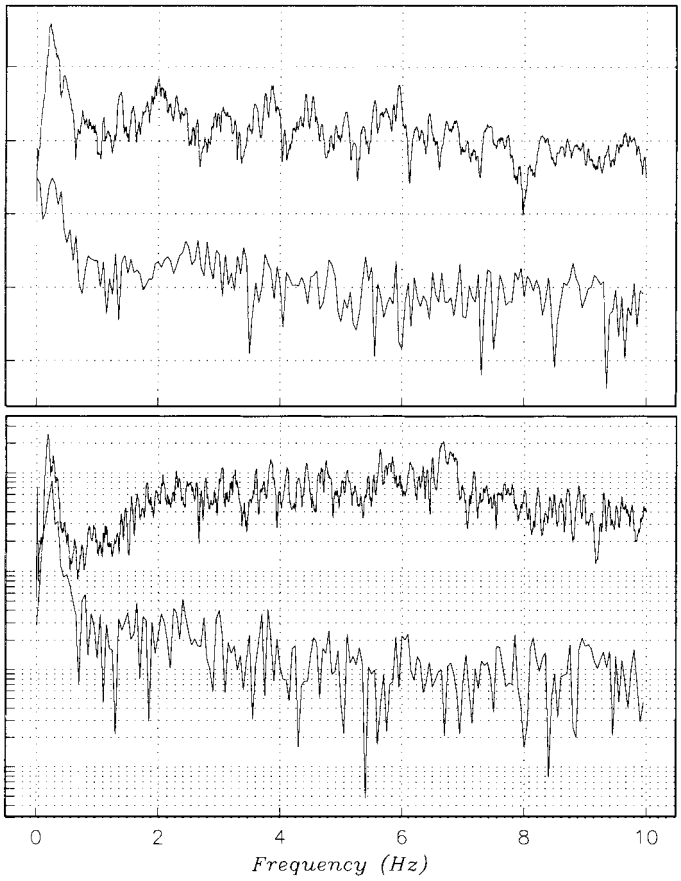

Figure 9
Spectral estimates taken from pre-event noise and signal recorded at CUST. In the upper panel, we display spectra taken from the recording of the July 19, 1996 cast blast (see Fig. 5). In the lower panel we display spectra taken from the CUST recording of the 16,000 pound calibration shot. The noise spectral estimates were untapered. Both *P*-wave spectra have been convolved with a boxcar function spanning 0.04 Hz to give a clearer view of the spectral modulations in the upper panel.

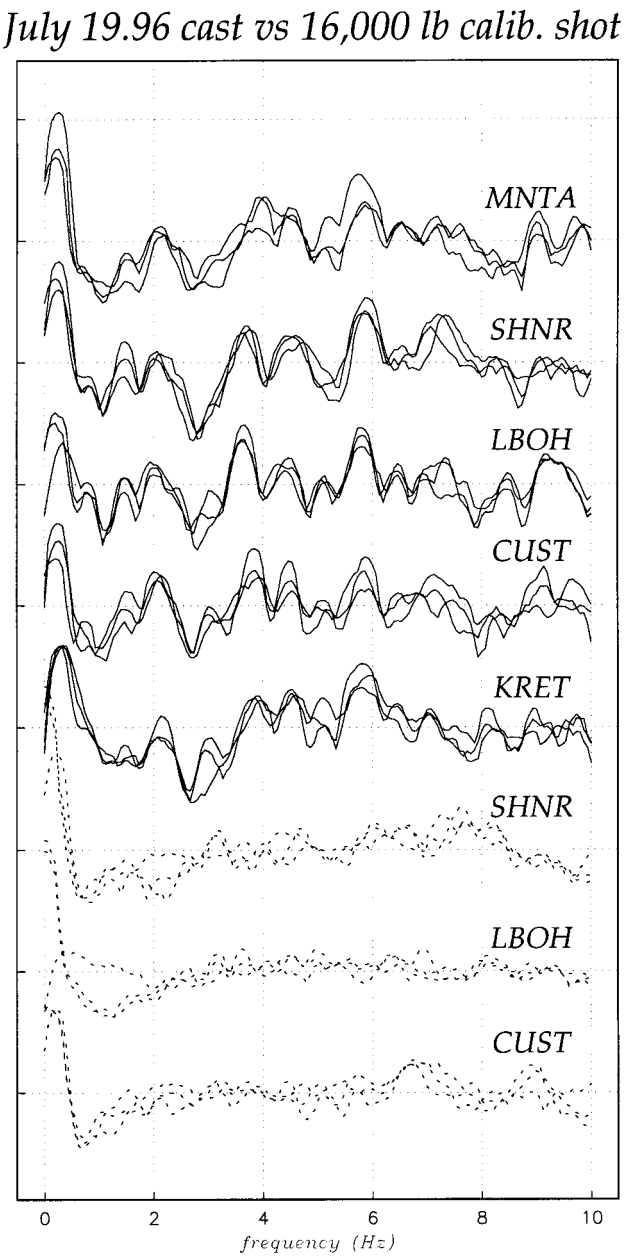

Figure 10
Obvious time-independent modulations exist below 10 Hz in the spectra of recordings of the July 19 cast blast (upper solid lines). At each station three curves, each representing the log of the spectral amplitude from a single component, are plotted. These are similar to the high-frequency modulations observed by HEDLIN *et al.* (1989) although these are likely due to source finiteness and interrow delays. Both these spectra and those observed by HEDLIN *et al.* (1989) are independent of the recording direction. A very slight dependence of the modulations on azimuth can be seen. The 16,000 pound calibration shot (dashed lines) produced no discernable spectral modulations. Each detrended multitaper spectral estimate was taken from 125 seconds of *P* and *S* coda. All components, from each three-component station, are plotted.

had a total yield of 0.0033 kt and thus the Sobel relation gives ~31 kt of spalled material. For the July 19 Black Thunder event we found this figure yielded surface waves that were more energetic than those that were recorded and so we reduced the spall figure to 20 kt. As will be discussed later, this discrepancy can be due to the incomplete conversion of spalled kinetic energy into seismic or to inadequacy of the velocity model. We assumed that the spalled material was cast at an angle 10° above the horizontal and fell 20 m.

Some vertical component synthetics are shown in Figure 11. This figure illustrates the relatively energetic surface waves that can be expected from cast blasts. The 16,000 pound point synthetic source, modeled as an isotropic source, produces a weak surface wave. The figure also illustrates the slow attenuation of the surface wave produced by the synthetic cast blast.

The peak amplitudes of the point source and the July 19, 1996 cast blast synthetics at a range of 200 km have been calculated for the four outer stations in the regional network (Fig. 3) and are displayed in Figure 8 with the observed amplitudes from the recorded events. Despite the assumptions listed above, we found the surface- and body-wave amplitudes produced by the synthetic event were consistent with the recorded waves at MNTA and CUST. The other two stations (LBOH and SHNR) yielded broadly dispersed surface waves which had lower peak amplitudes in the frequency band from 2 to 10 seconds. This pronounced mismatch is not due to unmodeled source effects but results from the propagation of the energy through a crust that differs significantly from the one-dimensional Prodehl model. Any comments at this time on what these differences imply about the crustal velocity model would be imprecise. A surface-wave inversion is currently being conducted by Rongmao Zhou and Brian Stump at Southern Methodist University. Although a significant azimuthal dependence of the surface-wave amplitudes is observed, the surface waves produced by the cast blasts are significantly more energetic at all azimuths than those produced by the single shots. The relatively minor azimuthal dependence that is seen in the synthetics is due to source directivity.

Experiments in Varying Source Parameters

Although we have reproduced the relative peak amplitudes of body and surface waves generated by the July 19 cast blast, several important questions remain unanswered. We have yet to determine which of the many source parameters included in the model play a leading role in generating the energetic surface waves. We need to gauge the sensitivity of the observed signals to changes in source parameters and to assess the utility of these signals for source characterization. ANANDAKRISHNAN *et al.* (1997) considered the effect of changes in several source parameters on regional waveforms. In this paper, we conduct a similar exercise; however, we are most interested in how these changes affect the partitioning of energy between the surface and body waves. We focus on the frequency bands considered in Figure 8. We

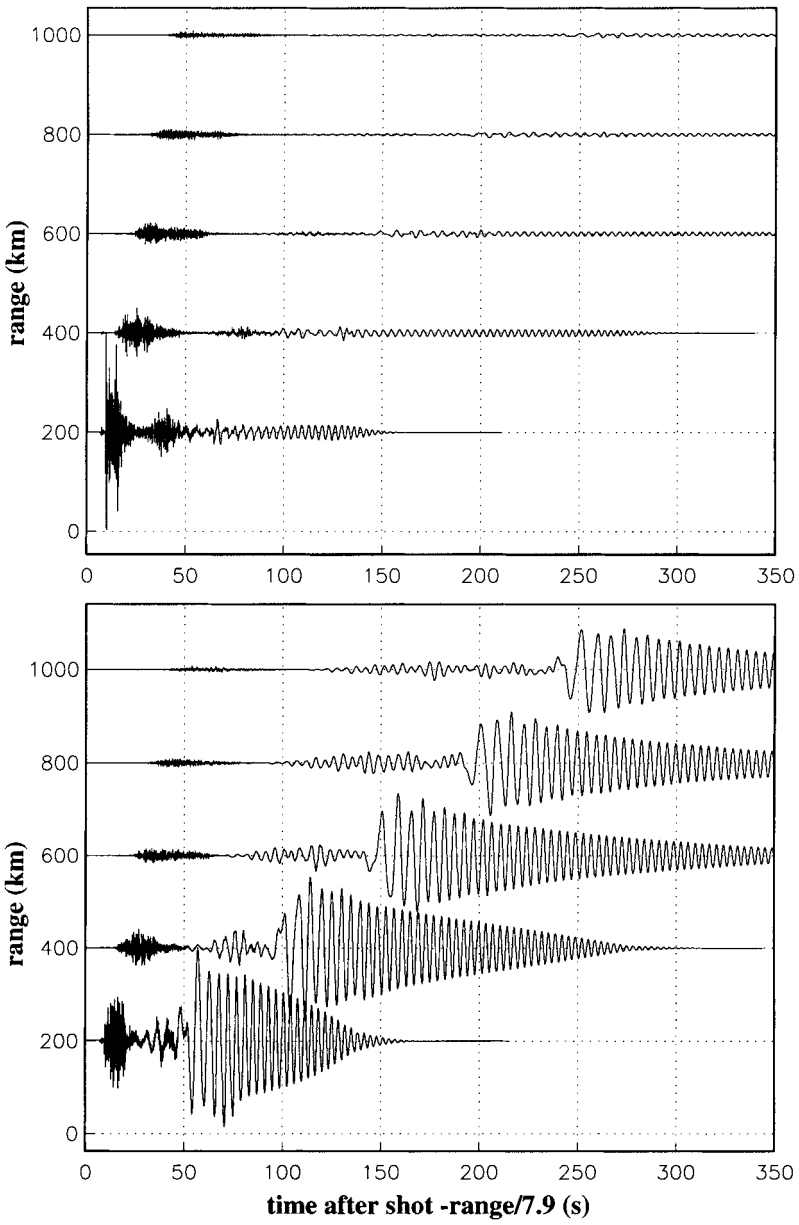

Figure 11

Simulations of two events. A single 16,000 lb shot is displayed on top, the July 19, 1996 cast shot is displayed on the bottom. The single shot is an insignificant source of surface waves. The surface waves excited by the cast blast decay relatively slowly and dominate the waveform of the cast shot at all ranges from 200 to 1000 km. The single shot synthetics are magnified for clarity. The range dependence of all synthetics was reduced by simply scaling all amplitudes by the range.

consider a broad suite of mine blasts. The blasts we synthesize are all the same as the presumed correct one reviewed in the previous section except one source parameter is allowed to vary while the others are held fixed. In turn, we vary the spalled mass, individual shot yield, and the duration of the blast. In a separate experiment we also allowed shot times to deviate from the planned 35 msec delays. All synthetics are calculated for CUST, the station located 200 km to the north of the mine. The results for the other three stations are essentially the same and are not plotted.

An example is shown in Figure 12 which displays synthetics for a suite of cast blasts in which the total yield of each shot hole is varied from 20% of the actual value to 200% (from 1468 to 14,676 pounds). The synthetics suggest that the body-wave amplitudes will scale rapidly with individual shot yield however the surface waves show a weaker dependence. This is consistent with ANANDAKRISHNAN *et al.* (1997) who concluded that the surface waves are mostly due to the different yield scaling in the explosion and spall source models.

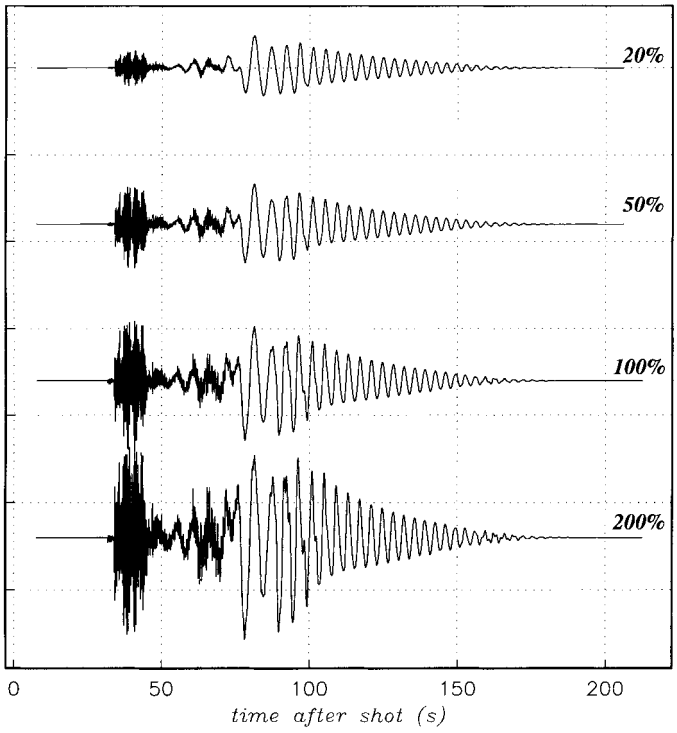

Figure 12
The dependence of vertical component waveforms on shot parameters is easily simulated using the MineSeis Matlab package. These plots show the dependence of the waveform on the yield of the individual shots. The standard cast, with individual shots of 7338 lb, is the third trace from the top. The scaling of the shot yield is indicated by the text to the right of each trace. The body-wave amplitudes depend strongly on shot yield. The surface waves show a weaker dependence.

A more general illustration of source effects on body and surface-wave amplitudes is given in Figure 13. In the upper panel of this figure we consider peak amplitudes in two filtered versions of the synthetic traces. We filter the synthetic traces between 2 and 10 s, and between 1 and 10 Hz and calculate the log of the peak amplitude in each trace. In Figure 13, we display the ratio of the peak amplitude in the the low-frequency trace to that in the high-frequency trace. In the upper panel, we

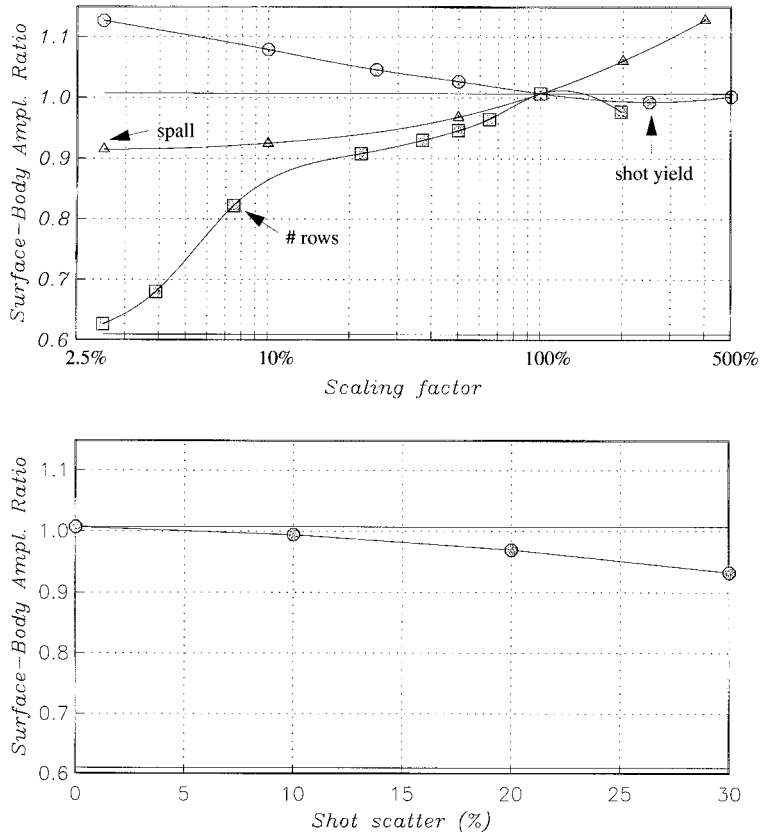

Figure 13

In the upper panel we display the surface-body wave ratios for a suite of blasts in which a single source parameter is varied while all others are held fixed at levels believed to be appropriate for the July 19, 1996 cast blast. The filled circles represent sources in which individual shot yield is varied from 182 to 36,300 lb. The filled triangles represent blasts in which the spalled mass per shot is varied from 0.5 kt to 80 kt. The squares represent blasts grids that range from a single row with three shots to a 10 row blast with 200 shots in each row. Varying blast duration clearly has the most significant impact on energy partitioning. Only the severely restricted grid partitions energy like the synthetic 16,000 pound shot (represented by the horizontal line at a ratio of 0.61). All of these simulations assumed the subshots detonated exactly when planned. The curve in the lower panel represents blasts in which the shot times are distributed normally about the planned times. The shot scatter considered ranges up a variance of 30% of the planned intershot delay of 35 msec.

display the ratios obtained from synthetic events in which a significant source parameter has been varied between 2.5% and 500% of the standard value. As seen in Figure 12, the surface wave to body-wave amplitude ratio decreases with increasing shot yield. This effect is represented by the filled circles in the upper panel of Figure 13. This effect is seen to be relatively minor as varying the yield over more than three orders of magnitude (from 182 to 36,300 pounds) changes the body-surface ratio by ~10%. As seen in Figure 12, this ratio change results from changes in both the surface- and body-wave amplitudes.

Varying the spalled mass has the opposite effect. When the spalled mass is varied from 0.5 kt to 80 kt (from 2.5% to 400% of the standard) the surface-body wave ratio changes from ~0.9 to 1.13 (filled triangles in the upper panel of Fig. 13). The change in this ratio results from the effect spalled mass has on the surface waves as the spalled mass is predominantly a source of low-frequency energy. Changing the spalled mass had little effect on the body-wave amplitudes. Although the production of surface waves is reduced when essentially no material is spalled into the pit, the restricted blast still produces surface waves that are significantly more energetic than those produced by the single shot.

The most significant changes in the waveform result from variations in the total duration of the blast. To vary the blast duration we scaled both the number of rows and the number of shots in each row. The standard blast had 7 rows and 89 shots in each row and lasted a total of ~4.8 s. The largest blast grid we considered had 10 rows, each with 200 shots. The extended blast spanned ~9.5 s – ~200% of the actual duration and had a total yield of 14 million pounds. The reduced blast grids consisted of 5 rows, 50 shots per row; 4 rows, 40 shots per row; 3 rows with 30 shots per row; 2 rows with 20 shots per row and 1 row with 10 shots. To reduce the blast further we decreased the number of shots in the final row to 5 shots and then to 3. The duration of these reduced blasts ranged from 3.1 s (for the blast with 5 rows and 50 shots per row) to 70 msec (for the smallest blast). As we see in Figure 13, extending the blast beyond the standard one that was used on July 19 yielded essentially no change in the surface-body wave amplitude ratio. However reducing the scale of the grid has a significant effect on the partitioning of energy between surface and body waves. Reducing the scale of the blast has a modest effect on body-wave amplitudes but the surface waves are strongly dependent on this source attribute. The ratio drops most rapidly when the blast duration is reduced below 2/10 of the actual duration (down to ~0.5 s from 4.8 s). The production of 2–10 s surface waves is reduced significantly when the blast duration is reduced below 2 seconds. When the blast duration extends much beyond 5 seconds, production of these surface waves is not increased substantially. Of all the blasts considered, just the brief blast resembled the single shot (which is represented by the horizontal line at a ratio of 0.61).

All synthetics considered thus far assumed a perfect temporal and spatial adherence of the actual shot grid to the design grid. Introducing shot time scatter, which is believed to be omnipresent (STUMP and REAMER, 1988; STUMP *et al.*, 1994,

1996), is predicted to have no effect on the surface-wave amplitudes but could increase the body-wave peak amplitudes significantly (Fig. 13; lower panel). Shot scatter increases the likelihood that shots will detonate simultaneously. An extreme example of shot scatter is the simultaneous detonation of a portion of the shot grid. This occurred in the August 1, 1996 blast and, as predicted by the synthetics, the surface waves were not affected (Fig. 8). The network averaged peak surface-wave amplitudes for the three mine blasts shown in this figure are very similar, despite the wide range of explosive yields. It appears that surface waves are just generated by temporally extensive mine blasts without regard for exactly how the blasts are detonated, and whether the blast sequence includes any significant detonation anomalies. The anomalous event was assigned a body wave magnitude of 4.0 (REB Bulletin).

5. Synthesis and Automated Recognition of Spectral Modulations

Synthesis

Seismic signals produced by delay-fired sources have spectral modulations at a wide range of frequencies. High-frequency modulations result directly from intershot delays. These delays are typically 35 msec and the modulations occur at multiples of 1/35 msec (~30 Hz). Interrow delays are typically longer. The cast blasts we consider in this paper have interrow delays of 200 to 300 msec which give modulations every ~3 to 5 Hz. Source finiteness will also cause subtle modulations spaced at the inverse of the duration of the event (e.g GITTERMAN and VAN ECK, 1993). Spectral modulations can also be acquired during propagation to the receiver (HEDLIN *et al.*, 1989). To illustrate this problem, and to illustrate the modulations that can result from source finiteness, we consider two synthetic sources – a single shot and a simple, 1 row, 25 shot delay-fired source. As shown in Figure 14, a single shot yields spectra with subtle modulations. These modulations are due to resonance in the near-surface layer of the model. This layer has a two-way travel time of ~0.4 s and thus produces modulations spaced at ~2.5 Hz. Much more significant modulations below 10 Hz are produced by the delay-fired event. The simple delay-fired event consisted of a single row of 25 shots. Intershot spacing of 35 msec produces a high-frequency modulation starting at 29 Hz (1/0.035 s). The shot sequence lasts for 0.875 s. The source finiteness causes a spectral modulation at the inverse of the source duration (peaks every 1.14 Hz).

To understand better the modulations produced by the July 19 event, we contrast signals from three different blasts with those produced by an instantaneous shot. Starting at the top of Figure 15, the upper three black traces are modulations between 1 and 10 Hz predicted for 1, 4 and 7 row cast blasts, respectively. These synthetic blasts are modeled after the July 19 decked blast, we have just altered the number of rows. The dashed spectra were taken from a synthetic 16,000 pound

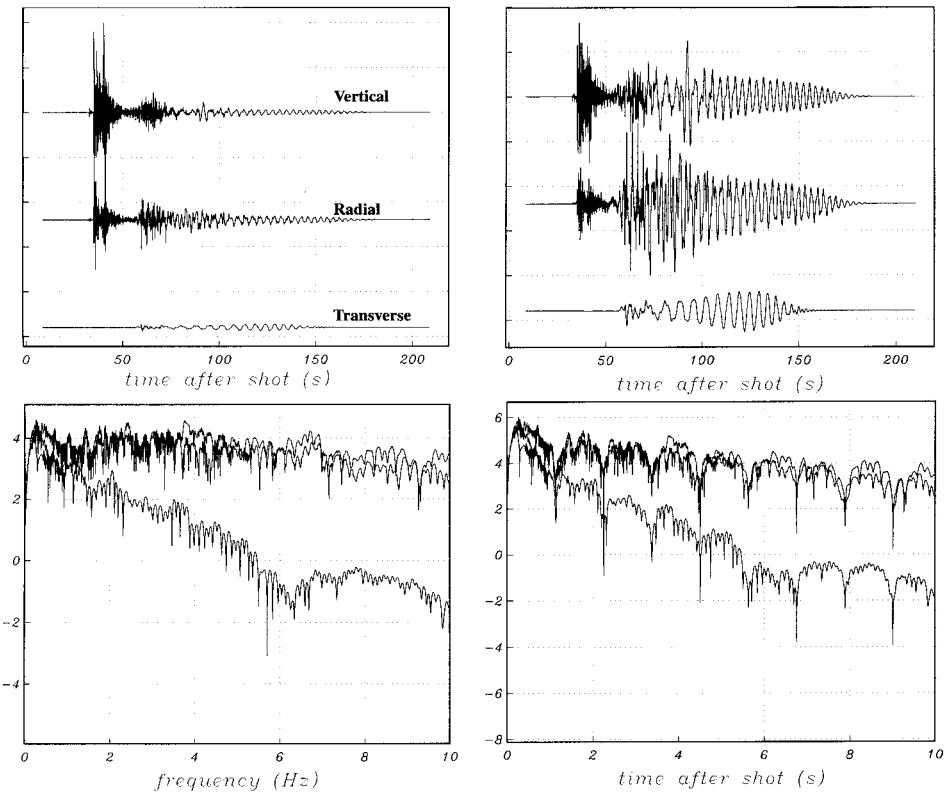

Figure 14
A synthetic 16,000 lb single shot at a range of 200 km is shown on the left. The faint spectral modulations seen in the spectra are due to resonance in near-surface low-velocity strata. A simple cast blast consisting of 1 row of 25 shots spaced at 35 msec is shown on the right. This simulation is for a station at a range of 200 km. The prominant modulations seen in the untapered spectral estimates are due to source finiteness. This shot lasted 0.875 s and produced modulations at the inverse of the duration (1.14 Hz). The first peak due directly to the intershot delays lies at 29 Hz.

instantaneous shot which was located at the same point. In the single row delay-fired event we see broad modulations spaced at ~2.5 Hz and fine-scale modulations spaced at ~0.3 Hz. The fine scale modulations are due to the finiteness of the source (which spanned ~3 s). The broader modulations are seen in the spectra from both sources and are due to resonance. Strong modulations spaced at ~0.75 Hz appear in the spectrum of the 7 row blast. These are not continuous across the band from 0 to 10 Hz but appear to be strongest at ~3 Hz. These modulations are not present in the spectra of the single-row blast and are due to the combined effect of the interrow and interdeck delays (which range from 0 to 300 msec) and source finiteness. Although the 7 row event had a total duration of ~5 s, the rate at which explosives were detonated was strongly dependent on time. The first shot in the final row detonated

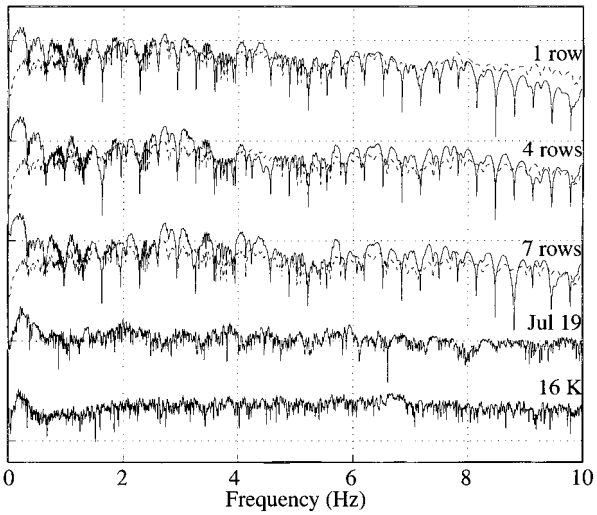

Figure 15
A comparison of spectra from synthetic and real events. The upper three black traces are vertical component spectra from synthetic cast blasts that are based on the July, 1996 south pit blast. The third spectrum is calculated from the full 7 row shot pattern. The middle and upper traces were calculated by using the front 4 and 1 rows, respectively. The grey curve plotted with each spectrum is from a synthetic 16,000 pound calibration shot. All synthetics were calculated for a receiver located 200 km to the north of the mine at the CUST station. The fourth spectrum is from the CUST vertical component of the July 19 event. The lowest trace is from the recorded 16,000 pound calibration shot. Broad modulations seen in all synthetic spectra result from resonance in the one-dimensional model. The fine-scale modulations are a source effect. Although the synthetics do not reproduce the fine detail of the low-frequency spectra recorded by the regional network, they do reproduce the general periodicity and variance of the modulations. In this figure, all spectral estimates are untapered.

$\sim$1.9 s after the shot sequence began. The final shot in the first row detonated $\sim$3.2 s into the sequence. For 1.3 s in the middle of the shot grid, all 7 rows were being detonated and the explosive yield per time delay was at a peak ($\sim$25,000 pounds per 8 msec delay period). The spectral modulations produced by this trapezoidal source time function are not spaced at the inverse of the total shot duration ($\sim$ every 0.2 Hz) but rather are more broadly spaced at $\sim$0.75 Hz (the inverse of the 1.3 s period during which explosive yield is at a peak). These fine scale modulations are not continuous across the band from 0 to 10 Hz because of destructive interference with long interrow and interdeck delays.

The fourth spectrum displayed in Figure 15 was taken from the vertical component recording of the July 19 event made at CUST. At the bottom of this figure we display a spectrum taken from the CUST recording of the 16,000 pound calibration shot. Strong peaks are observed in the cast blast spectrum at 2, 4, 6 and 10 Hz (see also Fig. 10). Smaller modulations are seen across the band from 1 to 10 Hz at a spacing of $\sim$0.75 Hz. These modulations are not seen in the spectrum of the calibration shot and are clearly a source effect. These modulations require source

delays of >1 s to 500 msec. The synthetic test displayed in the upper part of this figure suggests that these modulations are due to the combined effects of source finiteness and the complex interference between the 7 rows and 2 decks at this source; however, the fine spectral details are not reproduced.

We lack the necessary ground-truth information to reach definitive conclusions regarding probable causes of the mismatch between the observed and synthesized modulations; however, unmodeled source effects such as shot time and yield scatter seem most likely. The synthetic events we considered in this experiment consisted of shots that had exactly the same yield and detonated exactly when they were supposed to. Any deviations from uniform spacing of identical shots will change the manner in which signals from the different source processes (finiteness, interrow, interdeck and intershot delays) interfere with one another and will cause the recorded modulations to differ substantially from those predicted by synthetics. The synthetics suggest that most modulations observed in the recorded cast blast are due to long source delays and to source finiteness; however, this observation remains tentative as the fine details of the spectral modulations are not matched.

Automated Recognition

HEDLIN (1997, 1998a, b) used a variant of cepstral analysis to quantify time-independent spectral modulations at high frequencies (up to 40 Hz). The standard cepstrum is the Fourier transform of the log of a single spectrum. Hedlin used the two-dimensional Fourier transform of sonograms to isolate spectral energy that is periodic in frequency and independent of time. The same processing technique can be used for the low-frequency modulations observed here. Figure 16 shows discrimination parameters output by the Automated Time Frequency Discriminant (ATFD) for individual stations. The three parameters displayed are the autocorrelation, which measures the independence of spectral modulations with time; the cross correlation, which measures the independence from recording component; and cepstral extreme, which indicates the strength of time-independent spectral modulations. Although there were too few ground-truthed events to put the output to a statistical test, we tentatively conclude that the network averaged parameters separate single explosions from cast explosions.

6. IMS Recordings of the July 19, 1996 Cast Blast

The regional experiment provided evidence that large mining events will routinely yield significant low-frequency seismic signals. This network was deployed within 2° of the Powder River Basin so this test is rather unrealistic. Under a foreseeable monitoring scenario, where the bulk of the data comes from IMS stations, these events will be detected from mid-regional range. Detection statistics from the PIDC

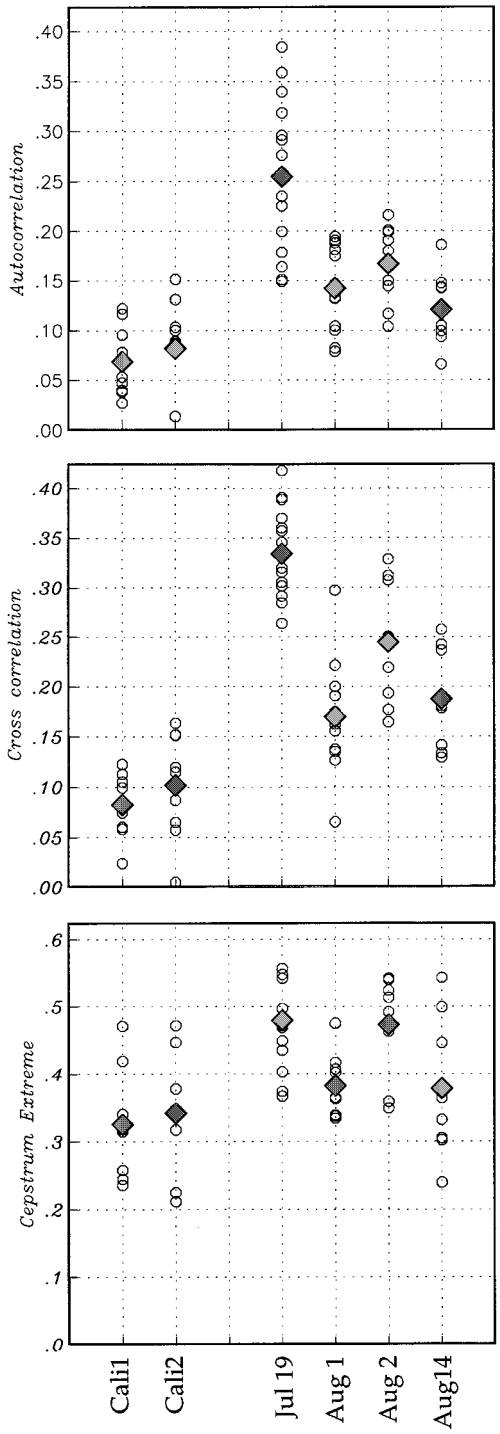
Autocorrelation
.40
.35
.30
.25
.20
.15
.10
.05
.00
Cross correlation
.40
.35
.30
.25
.20
.15
.10
.05
.00
Cepstrum Extreme
.6
.5
.4
.3
.2
.1
.0
Cali1
Cali2
Jul 19
Aug 1
Aug 2
Aug14

show that many of the PRB explosions are seen at far-regional to teleseismic range but can these attenuated signals be used for source characterization?

IMS recordings of the Wyoming events can give some indication of the range from which these signals might be used for source characterization. As shown in Figure 17, a low-frequency surface wave packet from the July 19, 1996 Black Thunder blast are seen out to ULM at a range of 9.1°. Figure 18 shows that the low-frequency spectral modulations also survive to this range; however, those above 6 Hz have fallen below noise.

7. Discussion and Conclusions

Mining Explosions and the CTBT

Under a CTBT, mining explosions will be problematic. As these events occur worldwide, many produce significant seismic signals which can be detected at mid- to far-regional and to teleseismic distances. Mining blasts are exceedingly complicated events. The complexity in the cast blasts considered in this paper stems primarily from the interaction of delay-fired explosives, rock fracture, and spall. The challenge mining events pose for the monitoring community is heightened because, through time, mine operators will occasionally experiment with new shot patterns. Furthermore, mine blasts will typically not detonate exactly as planned. Most deviations from the planned shot grid, such as shot scatter (e.g., STUMP and REAMER, 1988), are not highly significant. Other anomalies, such as the sympathetic detonations discussed in the introduction, are relatively infrequent but can be significant. A constraint is also placed on characterization methods by the IMS stations which sample the signal at 40 sps. Most diagnostic signals due to intershot delays are beyond the recording Nyquist frequency and are likely to be attenuated. For these reasons, we believe that it is important that a suite of approaches are developed to characterize these events. Under the CTBT, monitoring of mining blasts at any range will have to rely heavily on low-frequency signals.

◀

Figure 16

Discrimination parameters calculated by the Automated Time-Frequency Discriminant (ATFD, are described in detail in HEDLIN (1998). Each panel shows the results of applying a single operator to the time-frequency expansions of the data. The autocorrelation operator (top panel) assesses the dependance of the spectral modulation pattern on time. The cross correlation (middle panel) is a measure of the independence of the modulation pattern from the recording component. The cepstral extreme (bottom panel) is a measure of the amount of energy in the coda that is periodic in frequency and independant of time. Each three-component recording gives rise to nine parameters – three from each operator. Two calibration shots (left) and four cast blasts (right) were considered. The large symbols represent unweighted network averages.

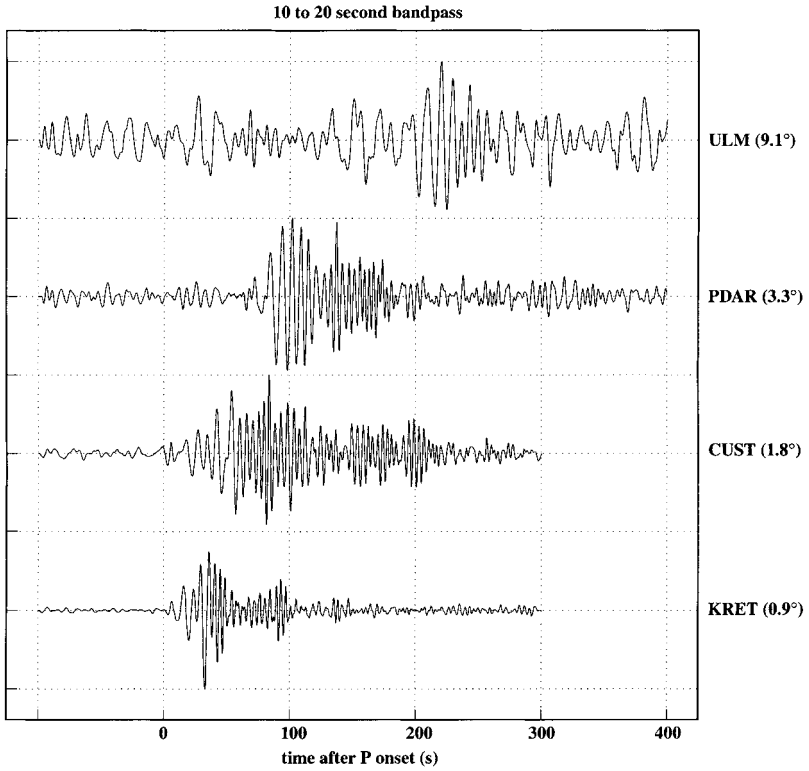

Figure 17
IMS/WYnet recordings of the Jul. 19, 1996 cast blast. The low-frequency bandpassed recordings exhibit an energetic dispersed surface wavetrain out to the IMS station ULM at 9.1°.

The Relative Merits of the Discriminants

Methods based on spectral modulations are potentially useful. For this approach to have value, it is necessary to separate modulations acquired at the source from those acquired during propagation and from those present in the background noise. Techniques that are dependent on high frequency modulations are typically limited to near-regional ranges and settings where the propagation Q is high (e.g., stable cratons). For this reason, this paper has focused on the causes of modulations below 10 Hz. It is apparent that complex mining blasts produce spectral modulations at a broad range of frequencies. The Wyoming field experiments have provided evidence that significant mining explosions will produce spectral modulations below 10 Hz that are not single-explosion like. Low-frequency modulations below 5 Hz will be detected beyond near-regional range. Just how common these signals are beyond near-regional range, and whether they are noticeable at lower blast yields is implied by our analysis of synthetics and by the recordings at ULM but will require further study of recorded events. The path from Wyoming to ULM probably has a relatively

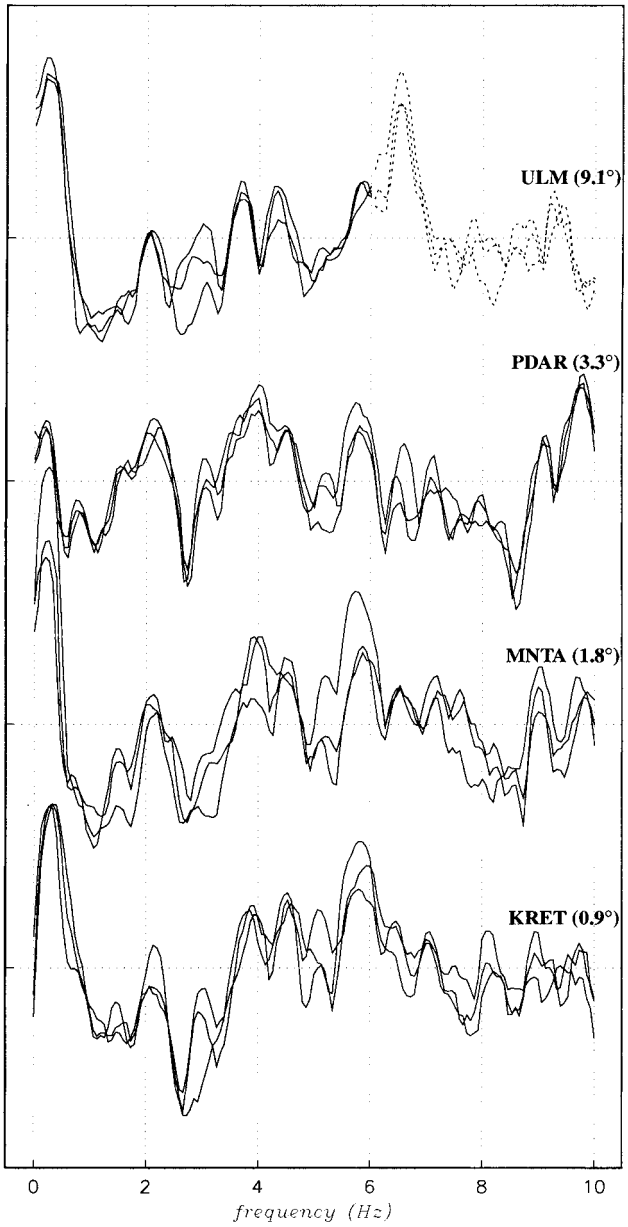

Figure 18
Multitaper spectral estimates taken from IMS and WYnet recordings the July 19 cast blast. The dashed portion of the ULM spectrum is noise. This robust low-frequency spectral roughness is not produced by small single explosions (Fig. 10).

high propagation Q. As a result, this observation cannot be taken as representative most regions but is the kind of scenario one might expect in a stable continental region. One region in which large mining blasts are not uncommon and propagation Q is relatively high is the Kuzbass/Abakan mining region in Kazakhstan. In regions where propagation Q is low, such as Wyoming, the high-frequency modulations due to intershot delays are quickly lost, although those due to longer duration source processes remain.

Long-period surface waves from large mining blasts in Wyoming are readily seen at mid-regional distances. The expenditure of a lot of energy spread out in time results in body waves that are relatively inenergetic and surface waves that are large. Our experiment indicates that the energy partitioning of mining blasts is not explosion-like and might be useful at mid-regional distances. It is clear that in geologically complex regions like Wyoming, surface waves are highly dependent on the path (Figs. 6–8). Even in this region, however, our study indicates that peak amplitudes along paths where surface waves are rapidly dispersed, are high.

Our analysis of a small number of events indicates that the observables (spectral roughness, energy partitioning) can be reduced to simple discrimination parameters. This result indicates that the ATFD approach developed by HEDLIN (1997, 1998a, b) can be simply scaled to lower frequencies where necessary. We have not yet attempted to define similar discrimination parameters for the body-surface amplitude ratios. In large part, this is due to a shortage of events included in the analysis and a shortage of recordings at ranges other than 200 km. A number of researchers (incl. ANANDAKRISHNAN *et al.*, 1997; STUMP and PEARSON, 1997) have pointed out anomalous surface waves. If this observation appears to be routine from studies of events from other regions the next logical step is to take source-receiver range into account and define a M_b:m_s relationship for mining blasts.

The potential for misidentifying a mining blast by using any one of these individual tools is rather high. It will, no doubt, be necessary to regionalize these techniques by examining, in detail, blasting practices and propagation in each area of interest. These tools will, perhaps, some day be used alongside other tools, such as cross correlation, that have been proven to be powerful by a number of researchers.

Simulations

The state-of-the-art in simulating mine blasts is not able to match wiggle for wiggle the seismic waves from these very complex events in the time or in the frequency domain. However, general features of these events (energy partitioning between body and surface waves, enhanced spectral roughness below 10 Hz) have been reproduced. We have used the synthetics as an interpretation tool to reproduce the general character of these events to better understand which source processes are important, but an exact replication might never be realized.

There are several likely causes of the misfit. The code makes a number of assumptions about these sources that limit how well we can fit the data. Nonlinear interactions between shots are not taken into account and are likely important (MINSTER and DAY, 1986). The model assumes 100% of the spall kinetic energy converts into seismic. It is known that much of this energy is used to compact the spalled mass by collapsing voids and fracturing the rock, more energy is irretrievably lost to friction; however, these losses are not well understood at this time and are not taken into account in this code. As a remedy, this loss of energy can be modeled to some degree by assigning a smaller amount of spalled mass. The spalled mass is directly proportional to the seismic energy the spall generates. All shots in the blast are assumed to be identical. However it is well known that explosive yield is highly variable. STUMP *et al.* (1999b, c) analyzed single-fired shots ranging in explosive weight from 5500 to 50,000 pounds. They found amplitudes from several 5000 pound shots varied by up to 2 orders of magnitude. The calibration shots considered by STUMP *et al.* (1999b, c) were, $\sim$30 m apart at the same vertical depth and so it is unlikely that changes in the physical properties of the medium are the cause of this variable performance. Velocity of detonation measurements in the holes were not made although video footage indicates a lot less borehole response in terms of motion and permanent displacement around the borehole for the event producing the smaller motions. These arguments support degraded explosive performance.

Other processes associated with each shot (e.g., spall tonnage and throw direction) are also assumed to be identical. Decorrelation between shots is also unavoidable (STUMP *et al.*, 1999b, c) and will degrade the constructive interference (BAUMGARDT, 1995). The analysis of single shots conducted by STUMP *et al.* (1999b, c) indicates that for the shot separations commonly used in these mining blasts ($\sim$10 m) we should expect good correlation below $\sim$4–5 Hz. Decorrelation is not taken into account in the current code as all sources are assigned a common Green's function. Shot timing is also an issue. We have concluded that low-frequency modulations result from long source delays and source finiteness; however, the fine details of these modulations are dependent on the interplay, or interference, between these processes. Marked changes in the modulation patterns can be caused by making seemingly minor adjustments in the shot pattern. Shot scatter, or the mismatch between intended and actual shot detonation times, is ever present (STUMP and REAMER, 1988) and is not taken into account in our simulations.

Despite these limitations, synthetics reproduce the general character of the spectral modulations observed and indicate that, in the absence of strong crustal resonance which will also yield spectral modulations, this trait can be useful for separating delay-fired blasts from instantaneous explosions. The synthetics underscore the need for taking into account seismic resonance. In the one-dimensional model, the low-velocity surface layer is continuous between the source and receiver. In practice, seismic resonance will be observed if the layer is discontinuous and present only at the source or at the receiver.

The energy partitioning between body and surface waves is more easily reproduced. The synthetic test clearly indicates that source duration has the most significant effect on surface wave amplitudes. Spall is a second-order effect. This successful simulation gives a physical basis to the surface waves observed. The source parameter tests are a first step in using synthetics to gauge the sensitivity of surface waves to changes at the source.

Outstanding Issues

This empirically based study has identified a number of characteristics of seismic waves from large-scale cast blasting that can be used for identifying the source. Within the context of the CTBT, the extent to which this observational experience can be used to assess discrimination techniques in other regions where propagation path effects are different and blasting practices may vary needs to be assessed. In some of these other areas there may be little or no access to information concerning blasting practices and so it is hoped that these detailed studies may provide the foundation for the interpretation of the observations after consideration of propagation path effects.

A number of outstanding issues associated with the generation of regional waveforms from mining explosions remain independent of specific information on propagation paths. Mechanisms for the generation of regional surface waves have been demonstrated but need further investigation and constraint. The impact of a range of blasting practices from long-time duration cast blasting in coal mines to short duration rock fragmentation blasts in surface coal mines needs to be explored. The modeling and data analysis have assumed that design blast parameters are those that are implemented. For purposes of assessing the reliability of discriminants, the quantification of anomalies in blasting and their implications for regional seismograms needs additional exploration. Finally this study has focused on observations from mining and single-fired explosions but has not compared these observations to those from earthquakes along similar propagation paths. Studies which include earthquake and mining explosion sources along comparable propagation paths will allow the assessment of the proposed discriminats for separating earthquake and mining explosion populations.

This study has focused on seismic observations from mining explosions. There is increasing evidence that infrasonic observations may help in the identification of surface mining explosions (SORRELLS *et al.*, 1997). It is possible that the colocation of seismic and infrasonic instrumentation surrounding mining regions may significantly add to the identification capability of mining explosions.

Mining events are controlled and thus might provide an opportunity for clandestine tests as part of an advanced nuclear weapons program. There is a strong incentive for learning how to use the IMS to distinguish anomalies from clandestine nuclear tests and avoid On-Site Inspections.

Unannounced mining events that include significant simultaneous explosive energy releases are problematic for several reasons. Such blasts are unwanted by the mining community as these events have both reduced rock-fracturing efficiency and increased seismic efficiency. Some of these blasts will trigger the IMS and cause some to question whether the anomalous energy release was chemical in nature. Effective characterization techniques, which rely on remote IMS observations, will reduce the need for on-site inspections. Our preliminary analysis suggests that such events can be identified using spectral modulations and the relative strength of surface- and body-wave seismic energy. A fuller analysis of errant blasts will be the subject of a forthcoming paper.

Acknowledgments

The combination of regional and close-in measurements for solving problems related to mining explosions could not have been made without the close collaboration with Vindell Hsu at the Air Force Technical Applications Center (AFTAC). Bob Martin, David Gross, Al Blakeman and Terry Walsh at the Black Thunder mine provided essential support. Portable deployments were made possible by CL Edwards, Diane Baker and Roy Boyd (LANL) and Adam Edelman, Aaron Geddins and John Unwin. The authors would like to thank Doug Baumgardt and an anonymous reviewer for helpful comments. Funding and equipment provided by LANL (under contracts 1973USML6-8F and F5310-0017-8F) and the efforts of Frank Vernon and the IGPP north lab permitted us to deploy the azimuthal network. Data processing and analysis by MAHH was funded by DTRA under contracts DTRA01-97-C-0153, and DTRA01-00-C-0115 and LANL under contract F5310-0017-8F.

References

Anandakrishnan, S., Taylor, S. R., and Stump, B. W. (1997), *Quantification and Characterization of Regional Seismic Signals from Cast Blasting in Mines: A Linear Elastic Model*, Geophys. J. Internat. *131*, 45–60.

Atlas Powder Company (1997), *Explosives and Rock Blasting*, Dallas, TX.

Barker, T. G. and Day, S. M. (1990), *A Simple Physical Model for Spall from Nuclear Explosions Based upon Two-dimensional Nonlinear Numerical Simulations*, PL Report SSS-TR-93-13859.

Barker, T. G., McLaughlin, K. L., Stevens, J. L., and Day, S. M. (1993), *Numerical Models of Quarry Blast Sources: The Effects of the Bench*, PL Semiannual Report, SSS-TR-93-13915.

Barker, T. G., McLaughlin, K. L., Stevens, J. L., and Day, S. M. (1994), *Numerical Simulation of Quarry Blasts Part 2: Implications for Discrimination*, Seismol. Res. Lett. *65*, 71.

Baumgardt, D. R. (1995), *Case Studies of Seismic Discrimination Problems and Regional Discriminant Transportability*, Phillips Lab Report PL-TR-95-2106.

Baumgardt, D. R. and Ziegler, K. A. (1988), *Spectral Evidence for Source Multiplicity in Explosions: Application to Regional Discrimination of Earthquakes and Explosions*, Bull. Seismol. Soc. Am. *78*, 1773–1795.

GITTERMAN, Y. and VAN ECK, T. (1993), *Spectra of Quarry Blasts and Microearthquakes Recorded at Local Distances in Israel*, Bull. Seismol. Soc. Am. *83*, 1799–1812.

GITTERMAN, Y., PINSKY, V., and SHAPIRA A. (1997), *Application of Spectral Semblance and Ratio Discriminants to Regional and Teleseismic Events Recorded by ISN and NORESS*, AFTAC/DOE/DSWA Seismol. Res. Symp. *19*, 369–378.

HARRIS, D. B. (1991), *A Waveform Correlation Method for Identifying Quarry Explosions*, Bull. Seismol. Soc. Am. *80*, 2177–2418.

HEDLIN, M. A. H. (1997), *A Global Test of a Time-frequency Small Event Discriminant*, AFTAC/DOE/DSWA Seism. Res. Symp. *19*, 390–399.

HEDLIN, M. A. H. (1998a), *Identification of Mining Blasts at all Regional Distances using Low-frequency Seismic Signals*, 20th Ann. Seis. Res. Symp. *20*, 335–344.

HEDLIN, M. A. H. (1998b), *A Global Test of a Time-frequency Small-event Discriminant*, Bull. Seismol. Soc. Am. *88*, 973–988.

HEDLIN, M. A. H., MINSTER, J.-B., and ORCUTT, J. A. (1989), *The Time-frequency Characteristics of Quarry Blasts and Calibration Explosions Recorded in Kazakhstan, U.S.S.R.*, Geophys. J. Int. *99*, 109–121.

ISRAELSSON, H. (1991), *Correlation of Waveforms from Closely Spaced Regional Events*, Bull. Seismol. Soc. Am. *80*, 6, 2177–2193.

KHALTURIN, V. I., RAUTIAN, T. G., RICHARDS, P. G., and KIM, W. Y. (1997), *Evaluation of Chemical Explosions and Methods of Discrimination for Practical Seismic Monitoring of a CTBT*, Phillips Lab. Final Report.

KIM, W. Y., SIMPSON, D. W., and RICHARDS, P. G. (1994), *High-frequency Spectra of Regional Phases from Earthquakes and Chemical Explosions*, *Bull. Seismol. Soc. Am. 84*, 1365–1386.

LANGEFORS, U. and KIHLSTRÖM, B. *The Modern Technique of Rock Blasting* (Halsted Press, Wiley, New York. 1978).

LEITH, W. (1994), *Large Chemical Explosions in the Former Soviet Union and Blasting Estimates for Countries of Nuclear Proliferation Concern*, Arms Control and Nonproliferation Technologies, 1st quarter 1994, 25.

MARTIN, R., GROSS, D., PEARSON, C., STUMP, B., and ANDERSON, D. (1997), *Black Thunder Coal Mine and Los Alamos Experimental Study of Seismic Energy Generated by Large-scale Mine Blasting*, Proc. Twenty-third Ann. Conf. on Explosives and Blasting Technique, Las Vegas, Nevada, Feb. 2–5, 1997, International Society of Explosive Engineers, Cleveland, Ohio*, pp. 1–10*.

MARTIN, R. L., and KING, M. G. (1995), *The Efficiency of Cast Blasting in Wide Pits*, Proc. Twenty-first Conf. on Explosives and Blasting Technique, Nashville, Tennessee, Feb. 5–9, 1995, International Society of Explosive Engineers, Cleveland, Ohio, pp. 176–186.

MCLAUGHLIN, K. L., BARKER, T. G., STEVENS, J. L., and DAY, S. M. (1994), *Numerical Simulation of Quarry Blast Sources*, PL Final Report SSS-FR-94-14418.

MINSTER, J.-B. and DAY, S. (1986), *Decay of Wavefields near an Explosive Source due to High-strain, Nonlinear Attenuation*, J. Geophys. Res. *91*, 2113–2122.

MURPHY, J. R. (1995), *Types of Seismic Events and their Source Description*, *Monitoring a Comprehensive Test Ban Treaty*, NATO ASI Series E: Applied Sciences, Vol. 303, (E. Husebye and A. Dainty ed.) 225–245.

PEARSON, D. C., STUMP, B. W., BAKER, D. F., and EDWARDS, C. L. (1995), *The LANL/LLNL/AFTAC Black Thunder Mine Regional Mining Blast Experiment*, 17th Annual PL/AFOSR/AFTAC/DOE Seism. Res. Symp., 562–571.

PRODEHL, C. (1979), *Crustal Structure of the Western United States*, US. Geological Survey Professional Paper, *1034*.

RICHARDS, P. G. and ZAVALES, J. (1990), *Seismic Discrimination of Nuclear Explosions*, Annu. Rev. Earth Planet. Sci. *18*, 257–286.

RIVIERE-BARBIER, F. and GRANT, L. T. (1993). *Identification and Location of Closely Spaced Mining Events*, Bull. Seismol. Soc. Am. *83*, 1527–1546.

SMITH, A. T. (1993), *Discrimination of Explosions from Simultaneous Mining Blasts*, Bull. Seismol. Soc. Am. *83*, 160–179.

SOBEL, P. A. (1978), *The Effect of Spall on m_b and M_s*, Teledyne Geotech Rept., SDAC-TR-77-12, Dallas, TX.

SORRELLS, G. G., HERRIN, E. T., and BONNER, J. L. (1997), *Construction of Regional Ground-truth Databases Using Seismic and Infrasound Data*, Seism. Res. Lett. *68*, 743–752.

STUMP, B. W. (1995), *Practical Observations of U.S. Mining Practices and Implications for CTBT Monitoring*, Phillips Lab Report, PL-TR-95-2108.

STUMP, B. W. and REAMER, S. K. (1988), *Temporal and Spatial Source Effects from Near-surface Explosions*, 10th Annual AFGS/DARPA Seism. Res. Symp., 95–113.

STUMP, G. W., RIVIERE-BARBIER, F., CHERNOBY, I., and KOCH, K. (1994), *Monitoring a Test-ban Treaty Presents Scientific Challenges*, EOS, Trans. of the Am. Geophys. *Union 75*, 265.

STUMP, B. W., ANDERSON, D. P., and PEARSON, D. C. (1996), *Physical Constraints on Mining Explosions: Synergy of Seismic and Video Data with 3-D Models*, *Seismol. Res. Lett. 67*, 9–24.

STUMP, B. W. and PEARSON, D. C. (1997), *Comparison of Single-fired and Delay-fired Explosions at Regional and Local Distances*, 19th Ann. Seism. Res. Symp., 668–677.

STUMP, B. W., HEDLIN, M. A. H., PEARSON, D. C., and HSU, V. (1999a), *Characterization of Mining Explosions at Regional Distances*, Rev. Geophys., in Review.

STUMP, B. W., PEARSON, D. C., and HSU, V. (1999b), *Empirical Scaling Relations for Contained Single-fired Chemical Explosions and Delay-fired Mining Explosions at Regional Distances*, 1999 SSA Meeting.

STUMP, B. W., PEARSON, D. C., and HSU, V. (1999c), *Empirical Scaling Relations for Contained Single-fired Chemical Explosions and Delay-fired Mining Explosions at Regional Distances*, 21st Ann Seism. Res. Symp., 764–772.

STUMP, B. W. and REAMER, S. K. (1988), *Temporal and Spatial Source Effects from Near-surface Explosions*, 10th Ann. AFGS/DARPA Seism. Res. Symp. *95*, 113.

U.S. CONGRESS, OFFICE OF TECHNOLOGY ASSESSMENT (1988), *Seismic Verification of Nuclear Testing Treaties*, OTA-ISC-361 (Washington, DC: U.S. Government Printing Office, May, 1988).

WUSTER, J., RIVIERE, F., CRUSEM, R., PLANTET, J. -L., MASSINON, B., and CARISTAN, Y. (2000), *GSETT-3: Evaluation of the Detection and Location Capabilities of an Experimental Global Seismic Monitoring System*, Bull. Seism. Soc. Am. *90*, 166–186.

YANG, X. (1998), *MineSeis – A Matlab GUI Program to Calculate Synthetic Seismograms from a Linear, Multi-Shot Blast Source Model*, 20th Ann. Seism. Res. Symp. 755–764.

(Received June 15, 1999, revised June 4, 2000, accepted June 15, 2000)